

The Dynamic Structures of the Type IV Pilus

MATTHEW MCCALLUM,^{1,2} LORI L. BURROWS,³
AND P. LYNNE HOWELL^{1,2}

¹Department of Biochemistry, University of Toronto, Toronto, ON M5S 1A8, Canada; ²Program in Molecular Medicine, Peter Gilgan Centre for Research and Learning, The Hospital for Sick Children, Toronto, ON M5G 0A4, Canada; ³Department of Biochemistry and Biomedical Sciences and the Michael G. DeGroot Institute for Infectious Disease Research, McMaster University, Hamilton, ON L8N 3Z5, Canada

ABSTRACT Type IV pilus (T4P)-like systems have been identified in almost every major phylum of prokaryotic life. They include the type IVa pilus (T4aP), type II secretion system (T2SS), type IVb pilus (T4bP), Tad/Flp pilus, Com pilus, and archaeal flagellum (archaellum). These systems are used for adhesion, natural competence, phage adsorption, folded-protein secretion, surface sensing, swimming motility, and twitching motility. The T4aP allows for all of these functions except swimming and is therefore a good model system for understanding T4P-like systems. Recent structural analyses have revolutionized our understanding of how the T4aP machinery assembles and functions. Here we review the structure and function of the T4aP.

INTRODUCTION

The fundamental type IVa pilus (T4aP)-like architecture includes a retractable pilus fiber, a motor, an alignment subcomplex, and—in Gram-negative bacteria—an outer membrane secretin pore (Fig. 1). The pilus is an extracellular polymer of pilins. Pilins subunits are stored in the inner membrane and the motor powers their polymerization (extension) and depolymerization (retraction) at the pilus base. The alignment subcomplex connects the secretin with the motor and controls pilus dynamics. Finally, the secretin pore allows the pilus to extend through the outer membrane. Since publication of previous T4aP reviews (1–4), discoveries made using cryo-electron microscopy (cryo-EM), cryo-electron tomography (cryo-ET), X-ray crystallography, and nuclear magnetic resonance (NMR) have dramatically reshaped our understanding of T4P-like systems. Here we put these discoveries in context

with the structure and function of the T4aP, using the *Pseudomonas aeruginosa* T4aP system nomenclature.

THE FIBER

The Major Subunit, PilA

The major pilin PilA is the most abundant subunit in the pilus fiber. X-ray crystallography (5–18) and NMR (19–21) structures revealed four typical features: an elongated S-shaped N-terminal α -helix (α 1N), a ~4-stranded antiparallel β -sheet, the $\alpha\beta$ -loop, and the D-loop (Fig. 2) (Table 1). The $\alpha\beta$ -loop and D-loop vary in sequence, structure, and posttranslational modifications between strains and species (7, 13, 18, 22–27). Together, the antiparallel β -sheet, $\alpha\beta$ -loop, and D-loop create a globular domain from which the α 1N helix protrudes. The hydrophobic α 1N helix retains pilins in the inner membrane

Received: 23 August 2018, **Accepted:** 2 January 2019,
Published: 1 March 2019

Editors: Maria Sandkvist, Department of Microbiology and Immunology, University of Michigan, Ann Arbor, Michigan; Eric Cascales, CNRS Aix-Marseille Université, Mediterranean Institute of Microbiology, Marseille, France; Peter J. Christie, Department of Microbiology and Molecular Genetics, McGovern Medical School, Houston, Texas

Citation: McCallum M, Burrows LL, Howell PL. 2019. The dynamic structures of the type IV pilus. *Microbiol Spectrum* 7(2):PSIB-0006-2018. doi:10.1128/microbiolspec.PSIB-0006-2018.

Correspondence: Lori L. Burrows, burrowl@mcmaster.ca; P. Lynne Howell, howell@sickkids.ca

© 2019 American Society for Microbiology. All rights reserved.

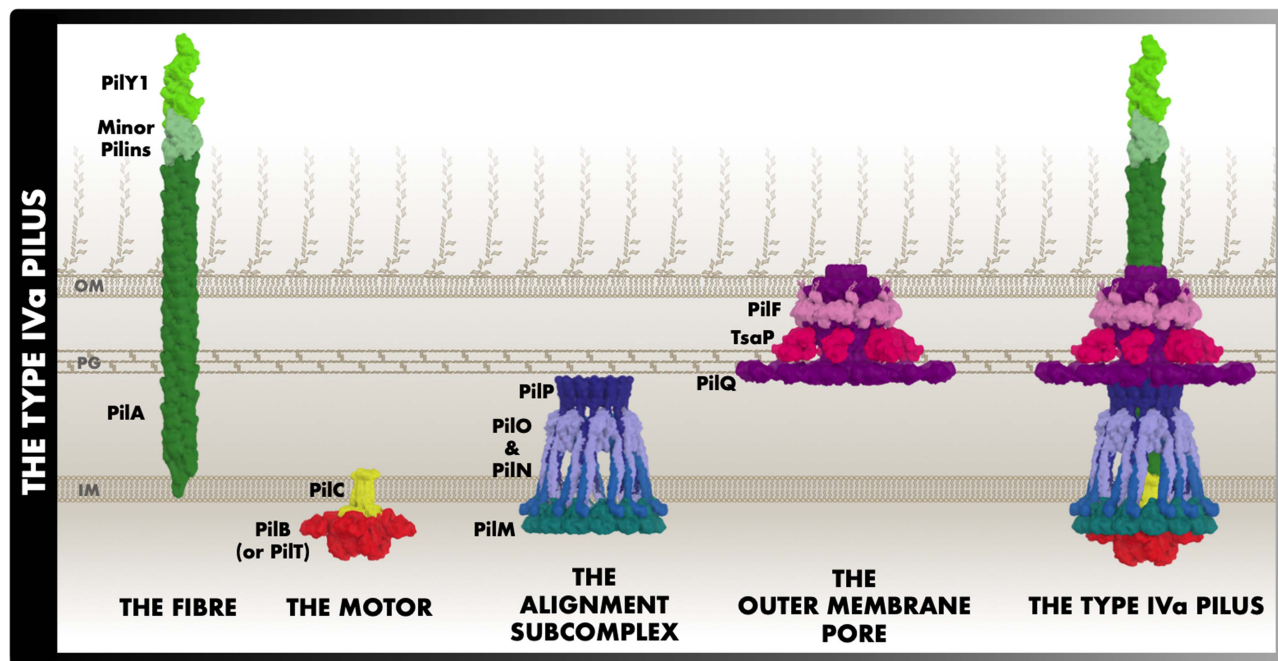


FIGURE 1 Subcomplexes of the T4aP. The protein structures portrayed reflect the full-length structure predictions and their predicted location in the T4aP. This figure is largely consistent with the previously published working model of the *M. xanthus* T4aP (43). Due to limited information, there is uncertainty regarding the locations of PilF, TsaP, PilY1, and the minor pilins.

prior to pilin polymerization and after pilin depolymerization. The peptidase PilD hydrolyzes the cytoplasmic leader sequence of nascent pilins and then methylates the new N terminus (28).

Recent 5- to 8-Å resolution cryo-EM maps of pilus fibers from *Neisseria* and *P. aeruginosa* (29, 30) largely validated older, lower-resolution models (6, 7, 13, 21, 31). With a helical rise of ~10 Å and 80 to 100° twist, the α1N helices bundle to form a hydrophobic core, while Glu-5 forms a salt bridge with the positively charged N-terminal amine of distal PilA molecules (6, 7, 13, 21, 29, 30). The αβ-loop and D-loop are surface exposed in these models, consistent with their sequence variability and posttranslational modifications that facilitate bacteriophage and immune evasion (6, 7, 24, 25). The 5- to 8-Å cryo-EM maps revealed that the segment between conserved Gly-14 and Pro-22 in the α1N helix was unexpectedly disordered in polymerized filaments (29, 30). This disordered region might allow the pilus to reversibly stretch to three times its original length (29, 32). Based on circular-dichroism analyses (33), the α1 helix is structured in pilin monomers (29, 30). Thus, relative to PilA monomers, the α1N in pilus fibers is stretched and may be under tension, or prestress—an architectural concept reviewed here (34), potentially explaining why the pilus appears to act more

like a rod than a rope in micrograph animations (35). Rod-like behavior could facilitate preferential adhesion of the pilus tip to substrates and twitching motility (36).

Minor Pilins

The low-abundance minor pilins are similar in architecture to PilA (37, 38). PilV, PilW, and PilX are functionally equivalent to GspI, GspJ, and GspK of the type II secretion system (T2SS), respectively (16, 39, 40). Crystallographic analysis of the globular domains of GspIJK heterotrimers revealed a helical arrangement of the three components with GspK at the tip (Fig. 2) (41). The bulky globular domain of GspK may hinder its insertion anywhere but at the pilus tip (41). This suggests that the GspIJK trimer, and by extension the PilVWX trimer, is located at the pilus tip, though PilX is less bulky than GspK (41). By self-assembling a short stem, minor pilins are thought to prime pilus assembly by reducing the energy barrier to extraction of pilins from the membrane (39, 41–43). Minor pilins FimU and PilE connect PilVWX to the PilA fiber (40, 44), and because they have the α1N helix-destabilizing Pro-22 residue missing in PilVWX (39, 40), they may initiate α1N helix melting during pilus assembly. Some T4aP include additional minor pilins with specialized binding capabili-

ties, like ComP in *Neisseria*, which binds DNA to promote uptake (38, 45–48).

PilY1

PilY1 is an adhesin that likely localizes to the pilus tip with PilVWX (39, 49, 50). The N-terminal region of PilY1 is variable and important for PilY1 adhesive capacities (49, 51). Crystallographic analyses revealed that the conserved C-terminal domain of PilY1 is a 7-bladed β -propeller domain with a calcium binding motif (51). Manipulation of this motif reduces PilY1-based adhesion in *Neisseria gonorrhoeae* (52) and causes retraction defects in *P. aeruginosa* (51).

THE MOTOR

PilC

PilC is a 3-pass inner membrane protein with two homologous globular cytoplasmic domains (53, 54) and, in many proteobacteria, a small cytoplasmic N-terminal domain with predicted $\beta\beta\alpha\beta$ topology (Fig. 2). Cryo-electron tomography (cryo-ET) of the *Myxococcus xanthus* T4aP machinery suggests that PilC is a dimer and localized in the pore of cytoplasmic hexameric ATPases PilB and PilT, while its transmembrane segments may interact with PilA (43). Given this organization, PilC might be rotated by PilB and PilT to catalyze PilA polymerization and depolymerization, respectively (43, 53). *In vitro* analyses support direct interactions between PilB and PilC, PilT and PilC, and PilA and PilC (53, 55–57). Purified PilC is dimeric and tetrameric, consistent with a 22-Å-resolution cryo-EM analysis of PilC from *Neisseria meningitidis* (54, 57, 58). The N-terminal domain of PilC from *Thermus thermophilus* was crystallized as an asymmetric homodimer, and mutating this dimer interface ablated *in vitro* tetramers but not dimers (54).

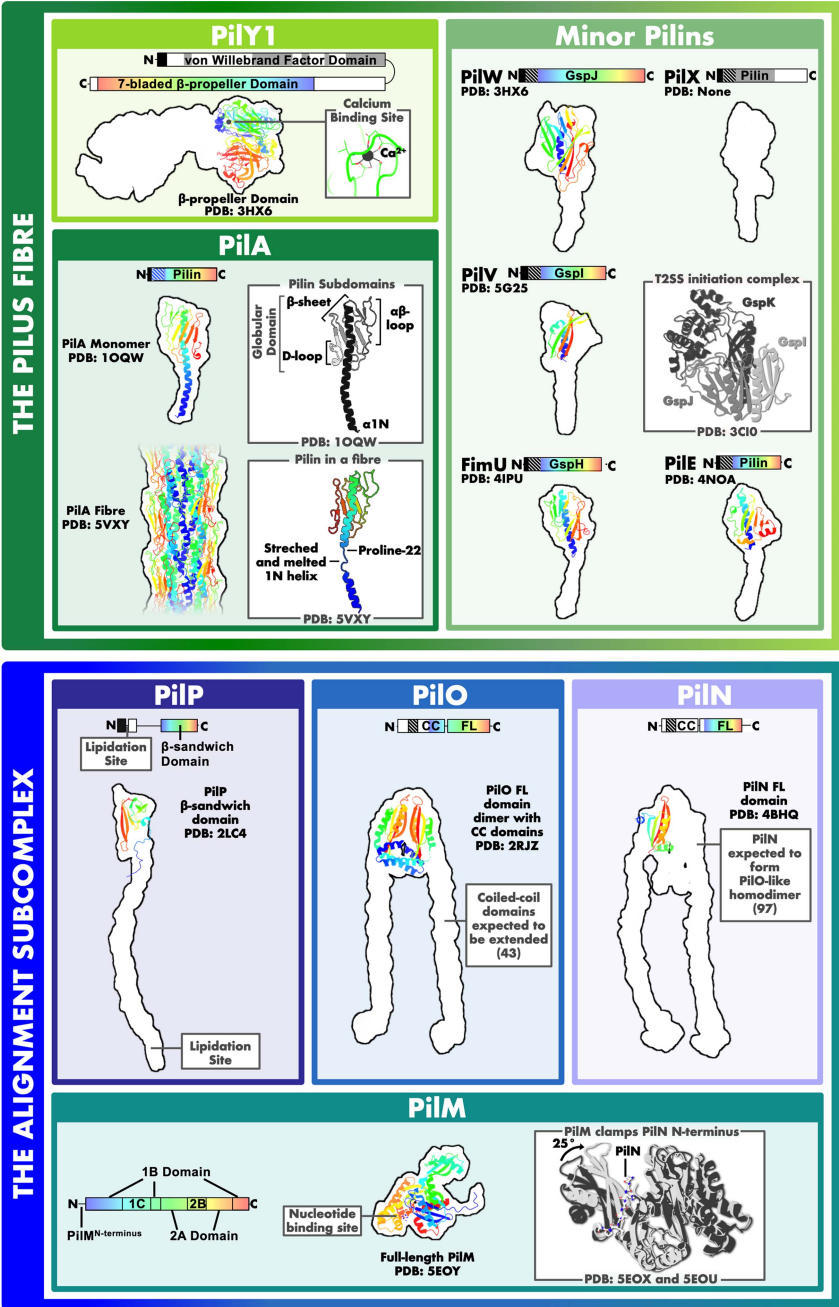
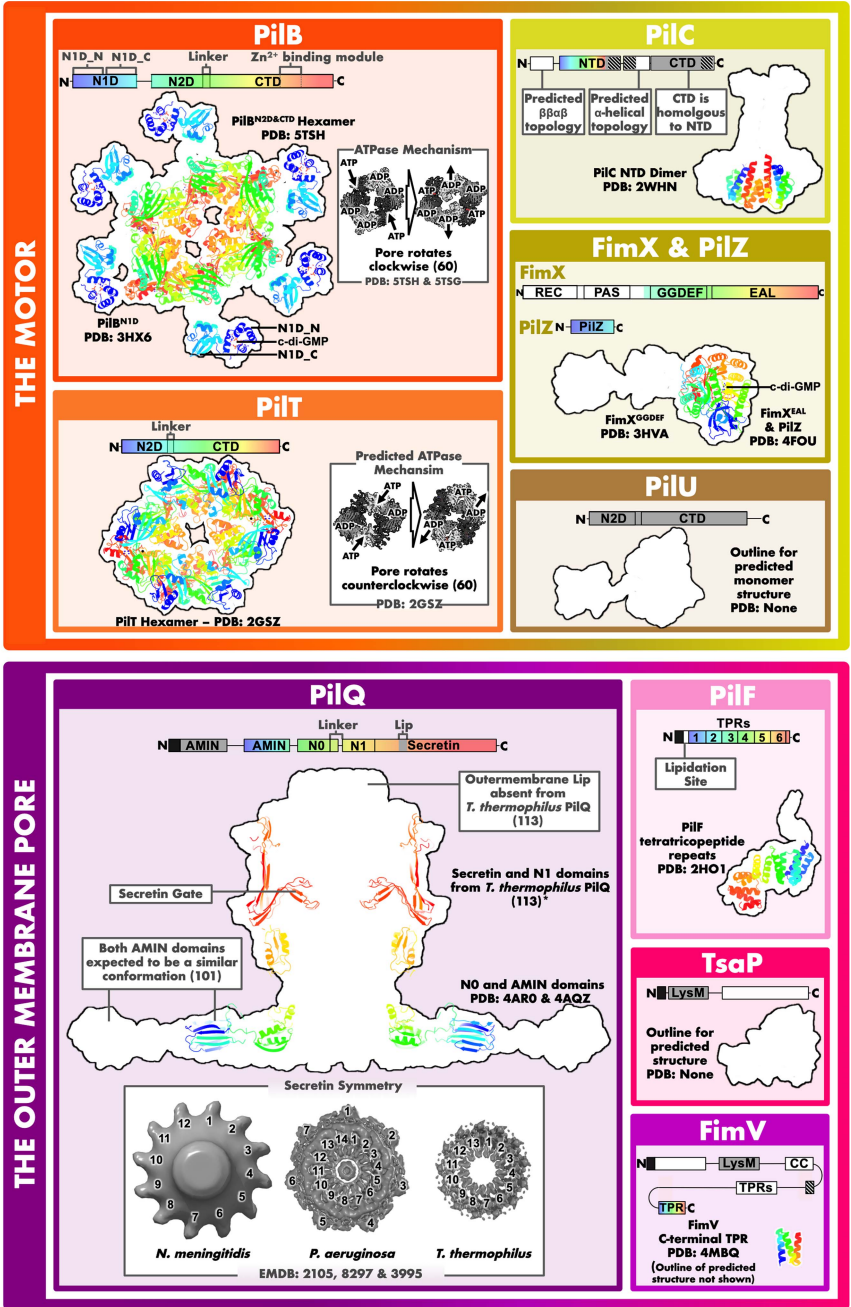
PilB and PilT

C_2 -symmetric structures of PilB from *T. thermophilus* (PilB^{Tt}) bound to the slowly hydrolyzable ATP analog ATP γ S (59), PilB from *Geobacter metallireducens* (PilB^{Gm}) bound to ADP plus the nonhydrolyzable ATP analog AMP-PNP (60), and apo-PilB from *Geobacter sulfurreducens* (PilB^{Gs}) (61) were recently determined. The symmetry of PilB^{Tt} initially suggested a C_2 rotary mechanism with a predicted counterclockwise pore rotation (59). In contrast, the two structures of PilB^{Gm} representing pre- and posthydrolysis states indicated a clockwise pore rotation (60) (Fig. 2) and that four of the six ATP γ S molecules in the lower-resolution PilB^{Tt} hexamer should have been modeled as ADP and mag-

nesium. We proposed that clockwise rotation of the PilB pore may move PilC clockwise in 60° increments to facilitate the polymerization of PilA into the right-handed helix observed by cryo-EM (29, 30, 60). Note that hydrolysis of ATP by PilB gives the impression of pore rotation, though PilB does not rotate during this process. Recent 8-Å resolution cryo-EM analysis of PilB^{Tt} showed a domain N terminal to the motor domains, the N1D, in a position that may block PilC from directly contacting the pore (62). Thus, the N1D might participate directly in the motor function of PilB (62). Alternatively, the N1Ds could regulate whether the PilB^{Tt} pore is available for binding PilC. Consistent with a rotary model, the PilB homolog from the archaeum FlaI is proposed to facilitate archaeum spinning; consistent with a C_2 -symmetric mechanism, purified FlaI, PilB, and PilT have two free ATP binding sites (61, 63–68).

The N1D of PilB is composed of two subdomains, N1D_N and N1D_C (69). The N1D_N subdomain of PilB binds the biofilm-related second messenger, c-di-GMP (69–71); the N1D_C subdomain also contacts c-di-GMP (69) (Fig. 2). A complex consisting of N1D_C of the T2SS PilB homolog, GspE, bound to the cytoplasmic domain of GspL (PilM) was crystallized (72, 73), suggesting a similar interaction in the T4aP (55). Therefore, c-di-GMP binding to PilB might regulate the PilB interaction with PilM and thus PilB engagement with the T4aP. PilB homologs from *P. aeruginosa*, *Xanthomonas campestris*, and *Xanthomonas axonopodis* lack an obvious c-di-GMP-binding motif in their N1D_N subdomains, though they interact with c-di-GMP-binding FimX, which also interacts with PilB-binding PilZ (74–76).

PilT is homologous to the motor domains of PilB and powers pilus depolymerization/retraction with extraordinary forces (35, 77–81). In addition to PilT, its paralogs in some T4aP systems, such as PilU, are also functionally significant (82–84). Pilus retraction is essential for several T4aP functions, including twitching motility, competence, and phage infection (77, 85, 86). In contrast to PilB, structures of PilT exhibit dissimilar rotational symmetries (87, 88). We applied the direction of ATP binding and hydrolysis of PilB to the structure of C_2 -symmetric PilT from *Aquifex aeolicus* (89) (Fig. 2). This analysis suggested that the pore and thus PilC would rotate counterclockwise to facilitate PilA depolymerization and pilus retraction (60). Intriguingly, the T4aP of *Vibrio cholerae* was recently reported to retract with low speed and force in a PilT knockout mutant (35), and the type IVb pilus (T4bP) systems of *V. cholerae* and the Tad pilus of *Caulobacter crescentus*, which lack retraction ATPases, were also reported to retract with low speed and force



(90, 91). Thus, PilT might simply enhance the speed and force of retraction (35). The energy for retraction in the absence of PilT was proposed to be potential energy stored in the pilus (90), possibly elastic tension in the melted α 1N helices of PilA (see above).

THE ALIGNMENT SUBCOMPLEX

PilM

Cryo-ET of *M. xanthus* indicated that PilM forms a ring on the inner leaflet of the inner membrane surrounding PilB or PilT (43), consistent with evidence that PilM binds to both PilB and PilT (53, 55, 57). The X-ray crystallographic structures of PilM from *T. thermophilus* and *P. aeruginosa* bound to the first eight residues of PilN have been solved, revealing that PilM is structurally similar to FtsA (55, 92). Interestingly, the T2SS homolog of PilM, GspL, is equivalent to a fusion of PilM and PilN (73, 92, 93). In the T4aP there is functional relevance for discrete PilM and PilN proteins, since PilN binding favors PilM-PilB interactions while reducing PilM-PilT interactions in bacterial two-hybrid experiments (55). Likewise, PilM subdomain 1C turns on a hinge to bind PilN (55) (Fig. 2), and this hinge is the predicted site for PilM-PilB interactions based on the homologous interactions in the T2SS (55, 72, 73). Thus, PilN binding to PilM might influence which ATPase is associated with the T4aP (55). Consistent with proposed conformational changes, the diameter of the PilM ring of *M. xanthus* is wider in the pilated than in the nonpilated state (43).

PilN and PilO

PilN and PilO are structurally similar inner membrane proteins with a cytoplasmic N-terminal peptide of ~20 residues, a transmembrane domain followed by a coiled-

coil domain, and a C-terminal globular domain with a ferredoxin-like fold (94–96). They form an oligomeric cage-like ring in the inner membrane and periplasm (43). The ferredoxin-like domains from *T. thermophilus* PilN and *P. aeruginosa* PilO crystallized as homodimers (94–96). One PilO structure from *P. aeruginosa* revealed a distinct PilO ferredoxin-like domain homodimer interface (95), and *in vivo* cysteine disulfide cross-linking studies of PilN and PilO homodimers and heterodimers are consistent with this interface (95–97). Cross-linked heterodimers, but not homodimers, interfere with T4aP function, suggesting that the homodimeric interface is stable while the heterodimeric interface may be dynamic (97). Mutagenesis studies suggest that heterodimerization occurs mainly through the coiled-coil domains, and coiled-coil mutations lead to pilus extension and retraction defects (98). Thus, PilN and PilO heterodimers are proposed to interact with PilM to influence which ATPase is bound (43, 55, 98).

PilP

PilP is an inner membrane lipoprotein with a partially disordered N-terminal region followed by a globular β -sandwich domain (99, 100). The partially disordered region binds to PilN and PilO heterodimers but not homodimers (100). Since heterodimeric PilN and PilO interactions are dynamic, the PilP interaction with PilN and PilO may also be dynamic (98). NMR analysis and pulldown experiments demonstrated that the β -domain of PilP also interacts with the N0 domain of PilQ, as do the homologous domains in the T2SS and T4bP (101–104). Thus, the PilMNOP subcomplex links the cytoplasmic ATPases to PilQ (43, 102). The dynamic interactions predicted for PilMNOP may also transduce signals. In *P. aeruginosa*, surface sensing is thought to

FIGURE 2 The structures of the type IV pilus. The four subcomplexes are split into four quadrants, which are further subdivided into individual proteins in boxes colored to correspond to Fig. 1. In the linear domain architecture, domains are displayed to scale as blocks colored to indicate known structures (rainbow colors), segments with high-confidence structure predictions (gray), unknown structures (white), transmembrane segments (diagonal bars), hydrolyzed signal peptides (black), or predicted/known disorder (black line). The known or predicted domain name is written; if a domain has no name, it could not be predicted. In the black outlined cartoon structures, a black outline of the predicted (127–129) full-length homology model is shown to scale for reference. Known structures are displayed as cartoons in rainbow colors corresponding to the colors shown in the linear domain architecture. A short description of the rainbow-colored cartoon structure and the PDB accession code are written in black font. Since the black outline is a *P. aeruginosa* structure prediction while the cartoons correspond to structures sometimes determined in other species, the black outline and cartoons may not fully match. Note that the PDB coordinate file for PilQ from *T. thermophilus* (marked with an asterisk) was obtained from the authors of reference 113 and used here with their permission; only the secretin and adjacent N1 domain (N5 in *T. thermophilus*) are shown here, as the other *T. thermophilus* PilQ domains are divergent or atypical compared to those in *P. aeruginosa*. (The N1 domain is also named N2, N3, N4, or N5 in systems or species where the N1 domain is duplicated.) No black outline is shown for FimV, as high-confidence structure prediction was not possible for most of this component. Unexpectedly, most of TsaP was predicted (127) with high confidence to be structurally similar to the protein with PDB code 3SLU. Gray boxes note interesting features of the protein or other relevant structures; structures in gray boxes are not to scale.

TABLE 1 List of available T4aP structures^a

<i>Pseudomonas</i> equivalent	Name	Species	PDB (EMDB) code(s)	Reference(s)
The pilus fiber				
PilY1	PilY1	<i>Pseudomonas aeruginosa</i> PAO1	3HX6	51
PilV	Tt1218	<i>Thermus thermophilus</i>	5G25	16
PilW	Tt1219	<i>Thermus thermophilus</i>	5G23, 5G24	16
FimU	FimU	<i>Pseudomonas aeruginosa</i> PAO1	4IPU, 4IPV	39
PilE	PilE	<i>Pseudomonas aeruginosa</i> PAO1	4NOA	40
	PilX	<i>Neisseria meningitidis</i>	2OPD, 2OPE	45
	PilV	<i>Neisseria meningitidis</i>	5V23, ^b 5V0M ^b	None
PilA	PilA	<i>Acinetobacter baumannii</i>	4XA2, 5VAW, ^b 5IHJ, 5CFV	8
	PilA	<i>Geobacter sulfurreducens</i>	2M7G	19
	PilA	<i>Pseudomonas aeruginosa</i> PAK	1DZO, 1OQW, 1X6P/Q/R/X/Y/Z	6 , 12 , 17
	PilA	<i>Pseudomonas aeruginosa</i> K122-4	1HPW, 1QVE, 1RG0	14 , 21
	PilA	<i>Pseudomonas aeruginosa</i> Pa110594	JYZ, 3JZZ	5
	PilA	<i>Pseudomonas aeruginosa</i> consensus	2PY0	11
	PilA1	<i>Clostridium difficile</i>	4TSM, 4OGM, 4PE2	9
	FimA	<i>Dichelobacter nodosus</i>	3SOK	10
	PilBac1	<i>Shewanella oneidensis</i>	4D40, 4US7	15
	PilE	<i>Francisella tularensis</i>	3SOJ	10
	PilE	<i>Neisseria gonorrhoeae</i>	1AY2, 2HI2, 2PIL	7 , 13 , 18
	PilE	<i>Neisseria meningitidis</i>	5JW8, 4V1J ^b	29
	Tt1221	<i>Thermus thermophilus</i> HB8	4BHR	94
PilA fiber	PilA	<i>Pseudomonas aeruginosa</i> PAK	5VXY (8740)	30
	PilA4	<i>Thermus thermophilus</i>	None (3024)	119
	PilE	<i>Neisseria gonorrhoeae</i>	5VXX (8739)	30
	PilE	<i>Neisseria gonorrhoeae</i>	2HIL (1236)	7
	PilE	<i>Neisseria meningitidis</i>	5KUA (8287)	29
None known	ComP	<i>Neisseria meningitidis</i>	2M3K, 5HZ7	38 , 48
	ComP	<i>Neisseria subflava</i>	2NBA	38
	PilJ	<i>Clostridium difficile</i>	4IXJ	37
	Tt1222	<i>Thermus thermophilus</i> HB8	5G2F	16
The motor				
PilB	PilB	<i>Geobacter metallireducens</i>	5TSG, 5TSH	60
	PilF	<i>Thermus thermophilus</i>	5IT5, 6EJF (3882), 6F8L (4194), (2222), (2223)	59 , 62 , 130
	PilB	<i>Geobacter sulfurreducens</i>	5ZFR	61
PilB (N1D)	MshE	<i>Vibrio cholerae</i> serotype O1	5HTL	69
PilT	PilT	<i>Pseudomonas aeruginosa</i> PAO1	3JVU, 3JVV	88
	PilT	<i>Aquifex aeolicus</i> strain VF5	2EWW, 2EWW, 2EYU, 2GSZ	89
	PilT4	<i>Geobacter sulfurreducens</i>	5ZFQ	61
	PilT2	<i>Thermus thermophilus</i>	5FL3 ^b	None
PilC	PilC	<i>Thermus thermophilus</i>	2WHN	54
FimX	FimX	<i>Pseudomonas aeruginosa</i> PAO1	4AGO, 3HV9, 3HVA, 3HV8, 4AFY, 4J40	135 , 136
	FimX	<i>Xanthomonas</i> sp.	4FOK, 4F3H	76 , 137
	PilZ	<i>Xanthomonas</i> sp.	3CNR, 3DSG	75 , 138
	FimX and PilZ	<i>Xanthomonas</i> sp.	4FOU, 4F48	76 , 137
The alignment complex				
PilM	PilM	<i>Pseudomonas aeruginosa</i> PAO1	5EOX, 5EOY, 5EQ6	55
PilM and PilN ^{cyto}	PilM and PilN ^{cyto}	<i>Pseudomonas aeruginosa</i> PAO1	5EOU	55
	PilM and PilN ^{cyto}	<i>Thermus thermophilus</i>	2YCH	92
	PilN	<i>Thermus thermophilus</i>	4BHQ	94
	PilO	<i>Pseudomonas aeruginosa</i> PAO1	2RJZ, 5UVR	95 , 96
PilMN, PilMNO, and PilMNOA	PilMN, PilMNO, and PilMNOA	<i>Thermus thermophilus</i>	None ^c (4157, 4157, 4159)	94
PilP	PilP	<i>Pseudomonas aeruginosa</i> PAO1	2LC4, 2Y4X, ^b 2Y4Y ^b	100
	PilP	<i>Neisseria meningitidis</i>	2IVW	99

(continued)

TABLE 1 List of available T4aP structures^a (*continued*)

<i>Pseudomonas</i> equivalent	Name	Species	PDB (EMDB) code(s)	Reference(s)
The outer membrane pore	PilQ	<i>Pseudomonas aeruginosa</i> PAO1	None (8297)	114
	PilQ	<i>Thermus thermophilus</i>	None ^c (3985, 3995, 3996, 3997, 3998)	113
	PilQ	<i>Candidatus pelagibacter</i>	None (8330)	117
PilQ and PilP	PilQ and PilP	<i>Neisseria meningitidis</i>	4AV2 (2105)	101
PilQ (N0 and linker from N0 to N1)	PilQ (N0 and linker from N0 to N1)	<i>Neisseria meningitidis</i>	4AR0	101
PilQ (AMIN)	PilQ (β2)	<i>Neisseria meningitidis</i>	4AQZ	101
PilF	PilF	<i>Pseudomonas aeruginosa</i> PAO1	2HO1, 2FI7	134 , 139
PilF	PilW	<i>Neisseria meningitidis</i>	2VQ2	126
FimV	FimV	<i>Pseudomonas aeruginosa</i> PAO1	4MBQ, 4MAL	140
<i>In situ</i> structures of the T4aP		<i>Myxococcus xanthus</i>	3JC8, 3JC9 (3247–3264)	43
		<i>Thermus thermophilus</i>	None (8224, 3021–3024)	118 , 119

^aThese are the published T4aP structures, not those from related T2SS, T4bP, Com pilus, Tad/Flp pilus, or archaeallum.

^bPeer-reviewed article describing the structure has not been published yet.

^cA model could be built into the density, but the model was not published to the Protein Data Bank.

initiate with PilY1, proceed through PilMNOP, require PilT, and ultimately activate the diguanylate cyclase SadC ([105–108](#)).

THE OUTER MEMBRANE PORE

PilQ

The secretin domain of PilQ forms the outer membrane pore, and until recently this domain resisted structure determination. The structures of the other PilQ subdomains were determined by NMR: one of two peptidoglycan-binding AMIN (β) domains located near the N terminus, the N0 domain, and the N1 domain ([101](#)). In *P. aeruginosa*, the AMIN domains localize PilQ to sites of cell division for preinstallation of the T4aP complex into the nascent septa of the daughter cells ([109](#)). Since the N0 domain of PilQ is bound by PilP (see above), PilQ recruits and localizes PilMNOP ([110](#), [111](#)). In the absence of an outer membrane, Gram-positive bacteria with T4aP mostly lack PilP and PilQ homologs ([112](#)).

Using single-particle cryo-EM, ~19-Å-, 7.4-Å-, and 7.0-Å-resolution maps of full-length PilQ from *N. meningitidis*, *P. aeruginosa*, and *T. thermophilus*, respectively, have been determined ([101](#), [113](#), [114](#)). Two-dimensional (2D) cryo-EM top views are also available for outer membrane-embedded *N. gonorrhoeae* and *N. meningitidis* PilQ ([115](#), [116](#)). These maps are 12-, 13-, or 14-fold symmetric, consistent with dodecamers, tridecamers, or tetradecamers ([101](#), [113](#), [114](#), [117](#)). Given that PilQ ultimately connects to hexameric ATPases in the cytoplasm via the alignment subcomplex, there may be stoichiometry mismatches between subcomplexes in some T4aP systems.

Two internal gates have been identified in PilQ: the secretin gate and the periplasmic gate ([43](#), [101](#), [113](#), [114](#), [118](#), [119](#)), although some cryo-EM maps are missing one or the other. Model building in the 7.0-Å-resolution *T. thermophilus* PilQ cryo-EM map was made possible by using homology models of new 3- to 4-Å-resolution GspD cryo-EM models ([113](#), [120–123](#)). Based on these models, it is clear how the secretin gate prevents leakage of molecules in the absence of the pilus ([113](#), [124](#)). The function of the periplasmic gate is less clear. The linker between the N0 domain and N1 domain forms the periplasmic gate in *T. thermophilus* PilQ, though this portion of PilQ shows limited homology to more typical T4aP systems ([113](#)). Since the gates must reorient during pilus extension and after retraction, it is conceivable that PilP binding to the N0 domain could sense these movements and transmit a signal to the cytoplasm via PilMNO.

PilF, Tsap, and FimV

The PG-binding protein FimV is widely distributed in T4aP systems ([125](#)) and was originally thought to be a PilQ-stabilizing protein, as mutants had reduced levels of PilQ ([126](#)). Recent data suggest that FimV plays a role in localizing PilQ and contributes to the expression of multiple T4aP proteins via a cAMP-dependent surface sensing mechanism ([109](#), [127–130](#)).

The PilF pilotin protein is required for stability, outer membrane localization, and multimerization of PilQ ([131–134](#)). PilF is a six-tetratricopeptide repeat lipoprotein localized to the outer membrane ([126](#), [134](#)). In the cryo-EM 2D class averages of *Neisseria* PilQ and the 3D reconstruction of *P. aeruginosa* PilQ, 7-fold symmetric spokes were detected around 14-fold symmetric PilQ ([114–116](#)).

In the *P. aeruginosa* 3D reconstruction, the spokes are localized to the inner leaflet of the outer membrane (114). Density consistent with these spokes was also present in cryo-ET images of *M. xanthus* T4aP and the 3D reconstruction of *N. meningitidis* PilQ (43, 101). Similar spokes in the T2SS correspond to the unrelated T2SS pilotin (120), suggesting the T4aP spokes could be PilF. Indeed, the spoke symmetry suggests that the spokes may simultaneously bind at least two PilQ protomers in the assembled secretin, potentially stabilizing nascent PilQ oligomers to assist PilQ multimerization. Alternatively, it has been proposed that the peptidoglycan-binding protein TsaP may form the spokes, since deleting TsaP from *M. xanthus* or *N. gonorrhoeae* causes the spokes to disappear (43, 116). It is possible that these spokes comprise multiple proteins.

CONCLUSION

Recent advances in cryo-EM and cryo-ET allow us to put crystallographic and NMR structures of individual T4aP components into biological context (Fig. 1). With these advances, new mysteries have emerged. For example, how does PilC interface with PilA and the pilus fiber in a way that facilitates extension and retraction yet opposes pilus shedding? Do the proposed dynamics in PilMNOPQ form a mechanical signal cascade? Structural insights from the T4aP will help rationalize new findings and expedite our understanding of other T4P-like systems.

ACKNOWLEDGMENTS

M.M. has been funded by graduate scholarships from the Canadian Institutes for Health Research (CIHR) and the Province of Ontario. P.L.H. is the recipient of a Canada Research Chair. This work was supported by grant MOP 93585 from CIHR to L.L.B. and P.L.H.

REFERENCES

- Craig L, Li J. 2008. Type IV pili: paradoxes in form and function. *Curr Opin Struct Biol* 18:267–277. <http://dx.doi.org/10.1016/j.sbi.2007.12.009>.
- Leighton TL, Buensuceso RN, Howell PL, Burrows LL. 2015. Biogenesis of *Pseudomonas aeruginosa* type IV pili and regulation of their function. *Environ Microbiol* 17:4148–4163. <http://dx.doi.org/10.1111/1462-2920.12849>.
- Ayers M, Howell PL, Burrows LL. 2010. Architecture of the type II secretion and type IV pilus machineries. *Future Microbiol* 5:1203–1218. <http://dx.doi.org/10.2217/fmb.10.76>.
- Hospenthal MK, Costa TRD, Waksman G. 2017. A comprehensive guide to pilus biogenesis in Gram-negative bacteria. *Nat Rev Microbiol* 15:365–379. <http://dx.doi.org/10.1038/nrmicro.2017.40>.
- Nguyen Y, Jackson SG, Aidoo F, Junop M, Burrows LL. 2010. Structural characterization of novel *Pseudomonas aeruginosa* type IV pilins. *J Mol Biol* 395:491–503. <http://dx.doi.org/10.1016/j.jmb.2009.10.070>.
- Craig L, Taylor RK, Pique ME, Adair BD, Arvai AS, Singh M, Lloyd SJ, Shin DS, Getzoff ED, Yeager M, Forest KT, Tainer JA. 2003. Type IV pilin structure and assembly: X-ray and EM analyses of *Vibrio cholerae* toxin-coregulated pilus and *Pseudomonas aeruginosa* PAK pilin. *Mol Cell* 11:1139–1150. [http://dx.doi.org/10.1016/S1097-2765\(03\)00170-9](http://dx.doi.org/10.1016/S1097-2765(03)00170-9).
- Craig L, Volkmann N, Arvai AS, Pique ME, Yeager M, Egelman EH, Tainer JA. 2006. Type IV pilus structure by cryo-electron microscopy and crystallography: implications for pilus assembly and functions. *Mol Cell* 23:651–662. <http://dx.doi.org/10.1016/j.molcel.2006.07.004>.
- Piepenbrink KH, Lillehoj E, Harding CM, Labonte JW, Zuo X, Rapp CA, Munson RS, Jr, Goldblum SE, Feldman MF, Gray JJ, Sundberg EJ. 2016. Structural diversity in the type IV pili of multidrug-resistant *Acinetobacter*. *J Biol Chem* 291:22924–22935. <http://dx.doi.org/10.1074/jbc.M116.751099>.
- Piepenbrink KH, Maldarelli GA, Martinez de la Peña CF, Dingle TC, Mulvey GL, Lee A, von Rosenvinge E, Armstrong GD, Donnenberg MS, Sundberg EJ. 2015. Structural and evolutionary analyses show unique stabilization strategies in the type IV pili of *Clostridium difficile*. *Structure* 23:385–396. <http://dx.doi.org/10.1016/j.str.2014.11.018>.
- Hartung S, Arvai AS, Wood T, Kolappan S, Shin DS, Craig L, Tainer JA. 2011. Ultrahigh resolution and full-length pilin structures with insights for filament assembly, pathogenic functions, and vaccine potential. *J Biol Chem* 286:44254–44265. <http://dx.doi.org/10.1074/jbc.M111.297242>.
- Kao DJ, Churchill ME, Irvin RT, Hodges RS. 2007. Animal protection and structural studies of a consensus sequence vaccine targeting the receptor binding domain of the type IV pilus of *Pseudomonas aeruginosa*. *J Mol Biol* 374:426–442. <http://dx.doi.org/10.1016/j.jmb.2007.09.032>.
- Hazes B, Sastry PA, Hayakawa K, Read RJ, Irvin RT. 2000. Crystal structure of *Pseudomonas aeruginosa* PAK pilin suggests a main-chain-dominated mode of receptor binding. *J Mol Biol* 299:1005–1017. <http://dx.doi.org/10.1006/jmbi.2000.3801>.
- Parge HE, Forest KT, Hickey MJ, Christensen DA, Getzoff ED, Tainer JA. 1995. Structure of the fibre-forming protein pilin at 2.6 Å resolution. *Nature* 378:32–38. <http://dx.doi.org/10.1038/378032a0>.
- Audette GF, Irvin RT, Hazes B. 2004. Crystallographic analysis of the *Pseudomonas aeruginosa* strain K122-4 monomeric pilin reveals a conserved receptor-binding architecture. *Biochemistry* 43:11427–11435. <http://dx.doi.org/10.1021/bi048957s>.
- Gorgel M, Ulstrup JJ, Bøggild A, Jones NC, Hoffmann SV, Nissen P, Boesen T. 2015. High-resolution structure of a type IV pilin from the metal-reducing bacterium *Shewanella oneidensis*. *BMC Struct Biol* 15:4. <http://dx.doi.org/10.1186/s12900-015-0031-7>.
- Karuppiah V, Thistlethwaite A, Derrick JP. 2016. Structures of type IV pilins from *Thermus thermophilus* demonstrate similarities with type II secretion system pseudopilins. *J Struct Biol* 196:375–384. <http://dx.doi.org/10.1016/j.jsb.2016.08.006>.
- Dunlop KV, Irvin RT, Hazes B. 2005. Pros and cons of cryocrystallography: should we also collect a room-temperature data set? *Acta Crystallogr D Biol Crystallogr* 61:80–87. <http://dx.doi.org/10.1107/S0907444904027179>.
- Forest KT, Dunham SA, Koomey M, Tainer JA. 1999. Crystallographic structure reveals phosphorylated pilin from *Neisseria*: phosphoserine sites modify type IV pilus surface chemistry and fibre morphology. *Mol Microbiol* 31:743–752. <http://dx.doi.org/10.1046/j.1365-2958.1999.01184.x>.
- Reardon PN, Mueller KT. 2013. Structure of the type IVa major pilin from the electrically conductive bacterial nanowires of *Geobacter sulfurreducens*. *J Biol Chem* 288:29260–29266. <http://dx.doi.org/10.1074/jbc.M113.498527>.
- Nguyen Y, Boulton S, McNicholl ET, Akimoto M, Harvey H, Aidoo F, Melacini G, Burrows LL. 2018. A highly dynamic loop of the *Pseudomonas aeruginosa* PA14 type IV pilin is essential for pilus assembly. *ACS Infect Dis* 4:936–943. <http://dx.doi.org/10.1021/acscinfecdis.7b00229>.

21. Keizer DW, Slupsky CM, Kalisiak M, Campbell AP, Crump MP, Sastry PA, Hazes B, Irvin RT, Sykes BD. 2001. Structure of a pilin monomer from *Pseudomonas aeruginosa*: implications for the assembly of pili. *J Biol Chem* 276:24186–24193. <http://dx.doi.org/10.1074/jbc.M100659200>.
22. Hegge FT, Hitchen PG, Aas FE, Kristiansen H, Løvold C, Egge-Jacobsen W, Panico M, Leong WY, Bull V, Virji M, Morris HR, Dell A, Koomey M. 2004. Unique modifications with phosphocholine and phosphoethanolamine define alternate antigenic forms of *Neisseria gonorrhoeae* type IV pili. *Proc Natl Acad Sci USA* 101:10798–10803. <http://dx.doi.org/10.1073/pnas.0402397101>.
23. Jennings MP, Jen FE, Roddam LF, Apicella MA, Edwards JL. 2011. *Neisseria gonorrhoeae* pilin glycan contributes to CR3 activation during challenge of primary cervical epithelial cells. *Cell Microbiol* 13:885–896. <http://dx.doi.org/10.1111/j.1462-5822.2011.01586.x>.
24. Harvey H, Bondy-Denomy J, Marquis H, Sztanko KM, Davidson AR, Burrows LL. 2018. *Pseudomonas aeruginosa* defends against phages through type IV pilus glycosylation. *Nat Microbiol* 3:47–52. <http://dx.doi.org/10.1038/s41564-017-0061-y>.
25. Gault J, Ferber M, Machata S, Imhaus AF, Malosse C, Charles-Orszag A, Millien C, Bouvier G, Bardiaux B, Pêhau-Arnaudet G, Klinge K, Podglajen I, Ploy MC, Seifert HS, Nilges M, Chamot-Rooke J, Duménil G. 2015. *Neisseria meningitidis* type IV pili composed of sequence invariable pilins are masked by multisite glycosylation. *PLoS Pathog* 11:e1005162. <http://dx.doi.org/10.1371/journal.ppat.1005162>.
26. Tan RM, Kuang Z, Hao Y, Lee F, Lee T, Lee RJ, Lau GW. 2015. Type IV pilus glycosylation mediates resistance of *Pseudomonas aeruginosa* to opsonic activities of the pulmonary surfactant protein A. *Infect Immun* 83:1339–1346. <http://dx.doi.org/10.1128/IAI.02874-14>.
27. Kus JV, Kelly J, Tessier L, Harvey H, Cvitkovitch DG, Burrows LL. 2008. Modification of *Pseudomonas aeruginosa* Pa5196 type IV pilins at multiple sites with d-Araf by a novel GT-C family arabinosyltransferase, TfpW. *J Bacteriol* 190:7464–7478. <http://dx.doi.org/10.1128/JB.01075-08>.
28. LaPointe CF, Taylor RK. 2000. The type 4 prepilin peptidases comprise a novel family of aspartic acid proteases. *J Biol Chem* 275:1502–1510. <http://dx.doi.org/10.1074/jbc.275.2.1502>.
29. Kolappan S, Coureuil M, Yu X, Nassif X, Egelman EH, Craig L. 2016. Structure of the *Neisseria meningitidis* type IV pilus. *Nat Commun* 7:13015. <http://dx.doi.org/10.1038/ncomms13015>.
30. Wang F, Coureuil M, Osinski T, Orlova A, Altindal T, Gesbert G, Nassif X, Egelman EH, Craig L. 2017. Cryoelectron microscopy reconstructions of the *Pseudomonas aeruginosa* and *Neisseria gonorrhoeae* type IV pili at sub-nanometer resolution. *Structure* 25:1423–1435.e4. <http://dx.doi.org/10.1016/j.str.2017.07.016>.
31. Folkhard W, Marvin DA, Watts TH, Paranchych W. 1981. Structure of polar pili from *Pseudomonas aeruginosa* strains K and O. *J Mol Biol* 149:79–93. [http://dx.doi.org/10.1016/0022-2836\(81\)90261-8](http://dx.doi.org/10.1016/0022-2836(81)90261-8).
32. Egelman EH. 2017. Cryo-EM of bacterial pili and archaeal flagellar filaments. *Curr Opin Struct Biol* 46:31–37. <http://dx.doi.org/10.1016/j.sbi.2017.05.012>.
33. Watts TH, Scraba DG, Paranchych W. 1982. Formation of 9-nm filaments from pilin monomers obtained by octyl-glucoside dissociation of *Pseudomonas aeruginosa* pili. *J Bacteriol* 151:1508–1513.
34. Ingber DE, Wang N, Stamenovic D. 2014. Tensegrity, cellular biophysics, and the mechanics of living systems. *Rep Prog Phys* 77:046603. <http://dx.doi.org/10.1088/0034-4885/77/4/046603>.
35. Ellison CK, Dalia TN, Vidal Ceballos A, Wang JC, Biaisi N, Brun YV, Dalia AB. 2018. Retraction of DNA-bound type IV competence pili initiates DNA uptake during natural transformation in *Vibrio cholerae*. *Nat Microbiol* 3:773–780. <http://dx.doi.org/10.1038/s41564-018-0174-y>.
36. de Haan HW. 2016. Modeling and simulating the dynamics of type IV pili extension of *Pseudomonas aeruginosa*. *Biophys J* 111:2263–2273. <http://dx.doi.org/10.1016/j.bpj.2016.09.050>.
37. Piepenbrink KH, Maldarelli GA, de la Peña CF, Mulvey GL, Snyder GA, De Masi L, von Rosenvinge EC, Günther S, Armstrong GD, Donnenberg MS, Sundberg EJ. 2014. Structure of *Clostridium difficile* PilJ exhibits unprecedented divergence from known type IV pilins. *J Biol Chem* 289:4334–4345. <http://dx.doi.org/10.1074/jbc.M113.534404>.
38. Berry JL, Xu Y, Ward PN, Lea SM, Matthews SJ, Pelicic V. 2016. A comparative structure/function analysis of two type IV pilin DNA receptors defines a novel mode of DNA binding. *Structure* 24:926–934. <http://dx.doi.org/10.1016/j.str.2016.04.001>.
39. Nguyen Y, Sugiman-Marangos S, Harvey H, Bell SD, Charlton CL, Junop MS, Burrows LL. 2015. *Pseudomonas aeruginosa* minor pilins prime type IVa pilus assembly and promote surface display of the PilY1 adhesin. *J Biol Chem* 290:601–611. <http://dx.doi.org/10.1074/jbc.M114.616904>.
40. Nguyen Y, Harvey H, Sugiman-Marangos S, Bell SD, Buensuceso RN, Junop MS, Burrows LL. 2015. Structural and functional studies of the *Pseudomonas aeruginosa* minor pilin, PilE. *J Biol Chem* 290:26856–26865. <http://dx.doi.org/10.1074/jbc.M115.683334>.
41. Korotkov KV, Hol WG. 2008. Structure of the GspK-GspI-GspJ complex from the enterotoxigenic *Escherichia coli* type 2 secretion system. *Nat Struct Mol Biol* 15:462–468. <http://dx.doi.org/10.1038/nsmb.1426>.
42. Cisneros DA, Bond PJ, Pugsley AP, Campos M, Francetic O. 2012. Minor pseudopilin self-assembly primes type II secretion pseudopilus elongation. *EMBO J* 31:1041–1053. <http://dx.doi.org/10.1038/emboj.2011.454>.
43. Chang YW, Rettberg LA, Treuner-Lange A, Iwasa J, Søgaard-Andersen L, Jensen GJ. 2016. Architecture of the type IVa pilus machine. *Science* 351:aad2001. <http://dx.doi.org/10.1126/science.aad2001>.
44. Giltner CL, Habash M, Burrows LL. 2010. *Pseudomonas aeruginosa* minor pilins are incorporated into type IV pili. *J Mol Biol* 398:444–461. <http://dx.doi.org/10.1016/j.jmb.2010.03.028>.
45. Helaine S, Dyer DH, Nassif X, Pelicic V, Forest KT. 2007. 3D structure/function analysis of PilX reveals how minor pilins can modulate the virulence properties of type IV pili. *Proc Natl Acad Sci U S A* 104:15888–15893. <http://dx.doi.org/10.1073/pnas.0707581104>.
46. Wolfgang M, van Putten JP, Hayes SF, Koomey M. 1999. The comp locus of *Neisseria gonorrhoeae* encodes a type IV prepilin that is dispensable for pilus biogenesis but essential for natural transformation. *Mol Microbiol* 31:1345–1357. <http://dx.doi.org/10.1046/j.1365-2958.1999.01269.x>.
47. Brown DR, Helaine S, Carbonnelle E, Pelicic V. 2010. Systematic functional analysis reveals that a set of seven genes is involved in fine-tuning of the multiple functions mediated by type IV pili in *Neisseria meningitidis*. *Infect Immun* 78:3053–3063. <http://dx.doi.org/10.1128/IAI.00099-10>.
48. Cehovin A, Simpson PJ, McDowell MA, Brown DR, Noschese R, Pallett M, Brady J, Baldwin GS, Lea SM, Matthews SJ, Pelicic V. 2013. Specific DNA recognition mediated by a type IV pilin. *Proc Natl Acad Sci U S A* 110:3065–3070. <http://dx.doi.org/10.1073/pnas.1218832110>.
49. Johnson MD, Garrett CK, Bond JE, Coggan KA, Wolfgang MC, Redinbo MR. 2011. *Pseudomonas aeruginosa* PilY1 binds integrin in an RGD- and calcium-dependent manner. *PLoS One* 6:e29629. <http://dx.doi.org/10.1371/journal.pone.0029629>.
50. Rudel T, Scheurerpflug I, Meyer TF. 1995. *Neisseria* PilC protein identified as type-4 pilus tip-located adhesin. *Nature* 373:357–359. <http://dx.doi.org/10.1038/373357a0>.
51. Orans J, Johnson MD, Coggan KA, Sperlazza JR, Heiniger RW, Wolfgang MC, Redinbo MR. 2010. Crystal structure analysis reveals *Pseudomonas* PilY1 as an essential calcium-dependent regulator of bacterial surface motility. *Proc Natl Acad Sci U S A* 107:1065–1070. <http://dx.doi.org/10.1073/pnas.0911616107>.
52. Cheng Y, Johnson MD, Burillo-Kirch C, Mocny JC, Anderson JE, Garrett CK, Redinbo MR, Thomas CE. 2013. Mutation of the conserved calcium-binding motif in *Neisseria gonorrhoeae* PilC1 impacts adhesion but not piliation. *Infect Immun* 81:4280–4289. <http://dx.doi.org/10.1128/IAI.00493-13>.

53. Takhar HK, Kemp K, Kim M, Howell PL, Burrows LL. 2013. The platform protein is essential for type IV pilus biogenesis. *J Biol Chem* 288: 9721–9728. <http://dx.doi.org/10.1074/jbc.M113.453506>.
54. Karupiah V, Hassan D, Saleem M, Derrick JP. 2010. Structure and oligomerization of the PilC type IV pilus biogenesis protein from *Thermus thermophilus*. *Proteins* 78:2049–2057.
55. McCallum M, Tammam S, Little DJ, Robinson H, Koo J, Shah M, Calmettes C, Moraes TF, Burrows LL, Howell PL. 2016. PilN binding modulates the structure and binding partners of the *Pseudomonas aeruginosa* type IVa pilus protein PilM. *J Biol Chem* 291:11003–11015. <http://dx.doi.org/10.1074/jbc.M116.718353>.
56. Georgiadou M, Castagnini M, Karimova G, Ladant D, Pelicic V. 2012. Large-scale study of the interactions between proteins involved in type IV pilus biology in *Neisseria meningitidis*: characterization of a subcomplex involved in pilus assembly. *Mol Microbiol* 84:857–873. <http://dx.doi.org/10.1111/j.1365-2958.2012.08062.x>.
57. Bischof LF, Friedrich C, Harms A, Søgaard-Andersen L, van der Does C. 2016. The type IV pilus assembly ATPase PilB of *Myxococcus xanthus* interacts with the inner membrane platform protein PilC and the nucleotide-binding protein PilM. *J Biol Chem* 291:6946–6957. <http://dx.doi.org/10.1074/jbc.M115.701284>.
58. Collins RF, Saleem M, Derrick JP. 2007. Purification and three-dimensional electron microscopy structure of the *Neisseria meningitidis* type IV pilus biogenesis protein PilG. *J Bacteriol* 189:6389–6396. <http://dx.doi.org/10.1128/JB.00648-07>.
59. Mancl JM, Black WP, Robinson H, Yang Z, Schubot FD. 2016. Crystal structure of a type IV pilus assembly ATPase: insights into the molecular mechanism of PilB from *Thermus thermophilus*. *Structure* 24:1886–1897. <http://dx.doi.org/10.1016/j.str.2016.08.010>.
60. McCallum M, Tammam S, Khan A, Burrows LL, Howell PL. 2017. The molecular mechanism of the type IVa pilus motors. *Nat Commun* 8:15091. <http://dx.doi.org/10.1038/ncomms15091>.
61. Solanki V, Kapoor S, Thakur KG. 2018. Structural insights into the mechanism of type IVa pilus extension and retraction ATPase motors. *FEBS J* 285:3402–3421. <http://dx.doi.org/10.1111/febs.14619>.
62. Collins R, Karupiah V, Siebert CA, Dajani R, Thistlethwaite A, Derrick JP. 2018. Structural cycle of the *Thermus thermophilus* PilF ATPase: the powering of type IVa pilus assembly. *Sci Rep* 8:14022. <http://dx.doi.org/10.1038/s41598-018-32218-3>.
63. Kinoshita Y, Uchida N, Nakane D, Nishizaka T. 2016. Direct observation of rotation and steps of the archaeum in the swimming halophilic archaeon *Halobacterium salinarum*. *Nat Microbiol* 1:16148. <http://dx.doi.org/10.1038/nmicrobiol.2016.148>.
64. Reindl S, Ghosh A, Williams GJ, Lassak K, Neiner T, Henche AL, Albers SV, Tainer JA. 2013. Insights into FlaI functions in archaeal motor assembly and motility from structures, conformations, and genetics. *Mol Cell* 49:1069–1082. <http://dx.doi.org/10.1016/j.molcel.2013.01.014>.
65. Alam M, Oesterheld D. 1984. Morphology, function and isolation of halobacterial flagella. *J Mol Biol* 176:459–475. [http://dx.doi.org/10.1016/0022-2836\(84\)90172-4](http://dx.doi.org/10.1016/0022-2836(84)90172-4).
66. Marwan W, Alam M, Oesterheld D. 1991. Rotation and switching of the flagellar motor assembly in *Halobacterium halobium*. *J Bacteriol* 173: 1971–1977. <http://dx.doi.org/10.1128/jb.173.6.1971-1977.1991>.
67. Shahapure R, Driessen RP, Haurat MF, Albers SV, Dame RT. 2014. The archaeum: a rotating type IV pilus. *Mol Microbiol* 91:716–723. <http://dx.doi.org/10.1111/mmi.12486>.
68. Chaudhury P, van der Does C, Albers SV. 2018. Characterization of the ATPase FlaI of the motor complex of the *Pyrococcus furiosus* archaeum and its interactions between the ATP-binding protein FlaH. *Peer J* 6:e4984. <http://dx.doi.org/10.7717/peerj.4984>.
69. Wang YC, Chin KH, Tu ZL, He J, Jones CJ, Sanchez DZ, Yildiz FH, Galperin MY, Chou SH. 2016. Nucleotide binding by the widespread high-affinity cyclic di-GMP receptor MshEN domain. *Nat Commun* 7: 12481. <http://dx.doi.org/10.1038/ncomms12481>.
70. Hendrick WA, Orr MW, Murray SR, Lee VT, Melville SB. 2017. Cyclic di-GMP binding by an assembly ATPase (PilB2) and control of type IV pilin polymerization in the Gram-positive pathogen *Clostridium perfringens*. *J Bacteriol* 199:e00034-17. <http://dx.doi.org/10.1128/JB.00034-17>.
71. Jones CJ, Utada A, Davis KR, Thongsomboon W, Zamorano Sanchez D, Banakar V, Cegelski L, Wong GC, Yildiz FH. 2015. C-di-GMP regulates motile to sessile transition by modulating MshA pili biogenesis and near-surface motility behavior in *Vibrio cholerae*. *PLoS Pathog* 11: e1005068. <http://dx.doi.org/10.1371/journal.ppat.1005068>.
72. Lu C, Korotkov KV, Hol WGJ. 2014. Crystal structure of the full-length ATPase GspE from the *Vibrio vulnificus* type II secretion system in complex with the cytoplasmic domain of GspL. *J Struct Biol* 187:223–235. <http://dx.doi.org/10.1016/j.jsb.2014.07.006>.
73. Abendroth J, Murphy P, Sandkvist M, Bagdasarian M, Hol WG. 2005. The X-ray structure of the type II secretion system complex formed by the N-terminal domain of EpsE and the cytoplasmic domain of EpsL of *Vibrio cholerae*. *J Mol Biol* 348:845–855. <http://dx.doi.org/10.1016/j.jmb.2005.02.061>.
74. Jain R, Shlusarenko O, Kazmierczak BI. 2017. Interaction of the cyclic-di-GMP binding protein FimX and the type 4 pilus assembly ATPase promotes pilus assembly. *PLoS Pathog* 13:e1006594. <http://dx.doi.org/10.1371/journal.ppat.1006594>.
75. Guzzo CR, Salinas RK, Andrade MO, Farah CS. 2009. PILZ protein structure and interactions with PilB and the FIMX EAL domain: implications for control of type IV pilus biogenesis. *J Mol Biol* 393:848–866. <http://dx.doi.org/10.1016/j.jmb.2009.07.065>.
76. Chin KH, Kuo WT, Yu YJ, Liao YT, Yang MT, Chou SH. 2012. Structural polymorphism of c-di-GMP bound to an EAL domain and in complex with a type II PilZ-domain protein. *Acta Crystallogr D Biol Crystallogr* 68:1380–1392. <http://dx.doi.org/10.1107/S0907444912030594>.
77. Merz AJ, So M, Sheetz MP. 2000. Pilus retraction powers bacterial twitching motility. *Nature* 407:98–102. <http://dx.doi.org/10.1038/35024105>.
78. Maier B, Potter L, So M, Long CD, Seifert HS, Sheetz MP. 2002. Single pilus motor forces exceed 100 pN. *Proc Natl Acad Sci U S A* 99: 16012–16017. <http://dx.doi.org/10.1073/pnas.242523299>.
79. Clausen M, Koomey M, Maier B. 2009. Dynamics of type IV pili is controlled by switching between multiple states. *Biophys J* 96:1169–1177. <http://dx.doi.org/10.1016/j.bpj.2008.10.017>.
80. Beaussart A, Baker AE, Kuchma SL, El-Kirat-Chatel S, O'Toole GA, Dufrene YF. 2014. Nanoscale adhesion forces of *Pseudomonas aeruginosa* type IV pili. *ACS Nano* 8:10723–10733. <http://dx.doi.org/10.1021/nn5044383>.
81. Clausen M, Jakovljevic V, Søgaard-Andersen L, Maier B. 2009. High-force generation is a conserved property of type IV pilus systems. *J Bacteriol* 191:4633–4638. <http://dx.doi.org/10.1128/JB.00396-09>.
82. Chiang P, Habash M, Burrows LL. 2005. Disparate subcellular localization patterns of *Pseudomonas aeruginosa* type IV pilus ATPases involved in twitching motility. *J Bacteriol* 187:829–839. <http://dx.doi.org/10.1128/JB.187.3.829-839.2005>.
83. Chiang P, Sampaleanu LM, Ayers M, Pahuta M, Howell PL, Burrows LL. 2008. Functional role of conserved residues in the characteristic secretion NTPase motifs of the *Pseudomonas aeruginosa* type IV pilus motor proteins PilB, PilT and PilU. *Microbiology* 154:114–126. <http://dx.doi.org/10.1099/mic.0.2007/011320-0>.
84. Kurre R, Höne A, Clausen M, Meel C, Maier B. 2012. PilT2 enhances the speed of gonococcal type IV pilus retraction and of twitching motility. *Mol Microbiol* 86:857–865. <http://dx.doi.org/10.1111/mmi.12022>.
85. Bradley DE. 1972. Shortening of *Pseudomonas aeruginosa* pili after RNA-phage adsorption. *J Gen Microbiol* 72:303–319. <http://dx.doi.org/10.1099/00221287-72-2-303>.
86. Wolfgang M, Lauer P, Park HS, Brossay L, Hébert J, Koomey M. 1998. PilT mutations lead to simultaneous defects in competence for natural transformation and twitching motility in pilated *Neisseria gonorrhoeae*. *Mol Microbiol* 29:321–330. <http://dx.doi.org/10.1046/j.1365-2958.1998.00935.x>.

87. Forest KT, Satyshur KA, Worzalla GA, Hansen JK, Herdendorf TJ. 2004. The pilus-retraction protein PilT: ultrastructure of the biological assembly. *Acta Crystallogr D Biol Crystallogr* 60:978–982. <http://dx.doi.org/10.1107/S0907444904006055>.
88. Mistic AM, Satyshur KA, Forest KT. 2010. *P. aeruginosa* PilT structures with and without nucleotide reveal a dynamic type IV pilus retraction motor. *J Mol Biol* 400:1011–1021. <http://dx.doi.org/10.1016/j.jmb.2010.05.066>.
89. Satyshur KA, Worzalla GA, Meyer LS, Heiniger EK, Aukema KG, Mistic AM, Forest KT. 2007. Crystal structures of the pilus retraction motor PilT suggest large domain movements and subunit cooperation drive motility. *Structure* 15:363–376. <http://dx.doi.org/10.1016/j.str.2007.01.018>.
90. Ng D, Harn T, Altindal T, Kolappan S, Marles JM, Lala R, Spielman I, Gao Y, Hauke CA, Kovacicova G, Verjee Z, Taylor RK, Biais N, Craig L. 2016. The *Vibrio cholerae* minor pilin TcpB initiates assembly and retraction of the toxin-coregulated pilus. *PLoS Pathog* 12:e1006109. <http://dx.doi.org/10.1371/journal.ppat.1006109>.
91. Ellison CK, Kan J, Dillard RS, Kysela DT, Ducret A, Berne C, Hampton CM, Ke Z, Wright ER, Biais N, Dalia AB, Brun YV. 2017. Obstruction of pilus retraction stimulates bacterial surface sensing. *Science* 358:535–538. <http://dx.doi.org/10.1126/science.aan5706>.
92. Karuppiah V, Derrick JP. 2011. Structure of the PilM-PilN inner membrane type IV pilus biogenesis complex from *Thermus thermophilus*. *J Biol Chem* 286:24434–24442. <http://dx.doi.org/10.1074/jbc.M111.243535>.
93. Abendroth J, Bagdasarian M, Sandkvist M, Hol WG. 2004. The structure of the cytoplasmic domain of EpsL, an inner membrane component of the type II secretion system of *Vibrio cholerae*: an unusual member of the actin-like ATPase superfamily. *J Mol Biol* 344:619–633. <http://dx.doi.org/10.1016/j.jmb.2004.09.062>.
94. Karuppiah V, Collins RF, Thistlethwaite A, Gao Y, Derrick JP. 2013. Structure and assembly of an inner membrane platform for initiation of type IV pilus biogenesis. *Proc Natl Acad Sci U S A* 110:E4638–E4647. <http://dx.doi.org/10.1073/pnas.1312313110>.
95. Sampaleanu LM, Bonanno JB, Ayers M, Koo J, Tammam S, Burley SK, Almo SC, Burrows LL, Howell PL. 2009. Periplasmic domains of *Pseudomonas aeruginosa* PilN and PilO form a stable heterodimeric complex. *J Mol Biol* 394:143–159. <http://dx.doi.org/10.1016/j.jmb.2009.09.037>.
96. Leighton TL, Mok MC, Junop MS, Howell PL, Burrows LL. 2018. Conserved, unstructured regions in *Pseudomonas aeruginosa* PilO are important for type IVa pilus function. *Sci Rep* 8:2600. <http://dx.doi.org/10.1038/s41598-018-20925-w>.
97. Leighton TL, Yong DH, Howell PL, Burrows LL. 2016. Type IV pilus alignment subcomplex proteins PilN and PilO form homo- and heterodimers in vivo. *J Biol Chem* 291:19923–19938. <http://dx.doi.org/10.1074/jbc.M116.738377>.
98. Leighton TL, Dayalani N, Sampaleanu LM, Howell PL, Burrows LL. 2015. A novel role for PilNO in type IV pilus retraction revealed by alignment subcomplex mutations. *J Bacteriol* 197:2229–2238. <http://dx.doi.org/10.1128/JB.00220-15>.
99. Golovanov AP, Balasingham S, Tzitzilonis C, Goult BT, Lian LY, Hombert H, Tønjum T, Derrick JP. 2006. The solution structure of a domain from the *Neisseria meningitidis* lipoprotein PilP reveals a new beta-sandwich fold. *J Mol Biol* 364:186–195. <http://dx.doi.org/10.1016/j.jmb.2006.08.078>.
100. Tammam S, Sampaleanu LM, Koo J, Sundaram P, Ayers M, Chong PA, Forman-Kay JD, Burrows LL, Howell PL. 2011. Characterization of the PilN, PilO and PilP type IVa pilus subcomplex. *Mol Microbiol* 82:1496–1514. <http://dx.doi.org/10.1111/j.1365-2958.2011.07903.x>.
101. Berry JL, Phelan MM, Collins RF, Adomavicius T, Tønjum T, Frye SA, Bird L, Owens R, Ford RC, Lian LY, Derrick JP. 2012. Structure and assembly of a trans-periplasmic channel for type IV pili in *Neisseria meningitidis*. *PLoS Pathog* 8:e1002923. <http://dx.doi.org/10.1371/journal.ppat.1002923>.
102. Tammam S, Sampaleanu LM, Koo J, Manoharan K, Daubaras M, Burrows LL, Howell PL. 2013. PilMNOPQ from the *Pseudomonas aeruginosa* type IV pilus system form a transenvelope protein interaction network that interacts with PilA. *J Bacteriol* 195:2126–2135. <http://dx.doi.org/10.1128/JB.00032-13>.
103. Korotkov KV, Johnson TL, Jobling MG, Pruneda J, Pardon E, Héroux A, Turley S, Steyaert J, Holmes RK, Sandkvist M, Hol WG. 2011. Structural and functional studies on the interaction of GspC and GspD in the type II secretion system. *PLoS Pathog* 7:e1002228. <http://dx.doi.org/10.1371/journal.ppat.1002228>.
104. Chang YW, Kjør A, Ortega DR, Kovacicova G, Sutherland JA, Rettberg LA, Taylor RK, Jensen GJ. 2017. Architecture of the *Vibrio cholerae* toxin-coregulated pilus machine revealed by electron cryotomography. *Nat Microbiol* 2:16269. <http://dx.doi.org/10.1038/nmicrobiol.2016.269>.
105. Kuchma SL, Ballok AE, Merritt JH, Hammond JH, Lu W, Rabinowitz JD, O'Toole GA. 2010. Cyclic-di-GMP-mediated repression of swarming motility by *Pseudomonas aeruginosa*: the *pilY1* gene and its impact on surface-associated behaviors. *J Bacteriol* 192:2950–2964. <http://dx.doi.org/10.1128/JB.01642-09>.
106. Luo Y, Zhao K, Baker AE, Kuchma SL, Coggan KA, Wolfgang MC, Wong GC, O'Toole GA. 2015. A hierarchical cascade of second messengers regulates *Pseudomonas aeruginosa* surface behaviors. *mBio* 6:e02456-14. <http://dx.doi.org/10.1128/mBio.02456-14>.
107. Siryaporn A, Kuchma SL, O'Toole GA, Gitai Z. 2014. Surface attachment induces *Pseudomonas aeruginosa* virulence. *Proc Natl Acad Sci U S A* 111:16860–16865. <http://dx.doi.org/10.1073/pnas.1415712111>.
108. Rodesney CA, Roman B, Dhamani N, Cooley BJ, Katira P, Touhami A, Gordon VD. 2017. Mechanosensing of shear by *Pseudomonas aeruginosa* leads to increased levels of the cyclic-di-GMP signal initiating biofilm development. *Proc Natl Acad Sci U S A* 114:5906–5911. <http://dx.doi.org/10.1073/pnas.1703255114>.
109. Carter T, Buensuceso RN, Tammam S, Lamers RP, Harvey H, Howell PL, Burrows LL. 2017. The type IVa pilus machinery is recruited to sites of future cell division. *mBio* 8:e02103-16. <http://dx.doi.org/10.1128/mBio.02103-16>.
110. Seitz P, Blokesch M. 2013. DNA-uptake machinery of naturally competent *Vibrio cholerae*. *Proc Natl Acad Sci U S A* 110:17987–17992. <http://dx.doi.org/10.1073/pnas.1315647110>.
111. Friedrich C, Bulyha I, Søgaard-Andersen L. 2014. Outside-in assembly pathway of the type IV pilus system in *Myxococcus xanthus*. *J Bacteriol* 196:378–390. <http://dx.doi.org/10.1128/JB.01094-13>.
112. Imam S, Chen Z, Roos DS, Pohlschröder M. 2011. Identification of surprisingly diverse type IV pili, across a broad range of gram-positive bacteria. *PLoS One* 6:e28919. <http://dx.doi.org/10.1371/journal.pone.0028919>.
113. D'Imprima E, Salzer R, Bhaskara RM, Sánchez R, Rose I, Kirchner L, Hummer G, Kühlbrandt W, Vonck J, Averhoff B. 2017. Cryo-EM structure of the bifunctional secretin complex of *Thermus thermophilus*. *eLife* 6:e30483. <http://dx.doi.org/10.7554/eLife.30483>.
114. Koo J, Lamers RP, Rubinstein JL, Burrows LL, Howell PL. 2016. Structure of the *Pseudomonas aeruginosa* type IVa pilus secretin at 7.4 Å. *Structure* 24:1778–1787. <http://dx.doi.org/10.1016/j.str.2016.08.007>.
115. Jain S, Mościcka KB, Bos MP, Pachulec E, Stuart MC, Keegstra W, Boekema EJ, van der Does C. 2011. Structural characterization of outer membrane components of the type IV pili system in pathogenic *Neisseria*. *PLoS One* 6:e16624. <http://dx.doi.org/10.1371/journal.pone.0016624>.
116. Siewering K, Jain S, Friedrich C, Webber-Birungi MT, Semchonok DA, Binzen I, Wagner A, Huntley S, Kahnt J, Klingl A, Boekema EJ, Søgaard-Andersen L, van der Does C. 2014. Peptidoglycan-binding protein TsaP functions in surface assembly of type IV pili. *Proc Natl Acad Sci USA* 111:E953–E961. <http://dx.doi.org/10.1073/pnas.1322889111>.

117. Zhao X, Schwartz CL, Pierson J, Giovannoni SJ, McIntosh JR, Nicastro D. 2017. Three-dimensional structure of the ultraoligotrophic marine bacterium “*Candidatus Pelagibacter ubique*.” *Appl Environ Microbiol* 83:e02807-16. <http://dx.doi.org/10.1128/AEM.02807-16>.
118. Salzer R, D’Imprima E, Gold VA, Rose I, Drechsler M, Vonck J, Averhoff B. 2016. Topology and structure/function correlation of ring- and gate-forming domains in the dynamic secretin complex of *Thermus thermophilus*. *J Biol Chem* 291:14448–14456. <http://dx.doi.org/10.1074/jbc.M116.724153>.
119. Gold VA, Salzer R, Averhoff B, Kühlbrandt W. 2015. Structure of a type IV pilus machinery in the open and closed state. *eLife* 4:e07380. <http://dx.doi.org/10.7554/eLife.07380>.
120. Yin M, Yan Z, Li X. 2018. Structural insight into the assembly of the type II secretion system pilotin-secretin complex from enterotoxigenic *Escherichia coli*. *Nat Microbiol* 3:581–587. <http://dx.doi.org/10.1038/s41564-018-0148-0>.
121. Hay ID, Belousoff MJ, Dunstan RA, Bamert RS, Lithgow T. 2018. Structure and membrane topography of the vibrio-type secretin complex from the type 2 secretion system of enteropathogenic *Escherichia coli*. *J Bacteriol* 200:e00521-17.
122. Hay ID, Belousoff MJ, Lithgow T. 2017. Structural basis of type 2 secretion system engagement between the inner and outer bacterial membranes. *mBio* 8:e01344-17. <http://dx.doi.org/10.1128/mBio.01344-17>.
123. Yan Z, Yin M, Xu D, Zhu Y, Li X. 2017. Structural insights into the secretin translocation channel in the type II secretion system. *Nat Struct Mol Biol* 24:177–183. <http://dx.doi.org/10.1038/nsmb.3350>.
124. Seike K, Yasuda M, Hatazaki K, Mizutani K, Yuhara K, Ito Y, Fujimoto Y, Ito S, Tsuchiya T, Yokoi S, Nakano M, Deguchi T. 2016. Novel *penA* mutations identified in *Neisseria gonorrhoeae* with decreased susceptibility to ceftriaxone isolated between 2000 and 2014 in Japan. *J Antimicrob Chemother* 71:2466–2470. <http://dx.doi.org/10.1093/jac/dkw161>.
125. Semmler AB, Whitchurch CB, Leech AJ, Mattick JS. 2000. Identification of a novel gene, *fimV*, involved in twitching motility in *Pseudomonas aeruginosa*. *Microbiology* 146:1321–1332. <http://dx.doi.org/10.1099/00221287-146-6-1321>.
126. Trindade MB, Job V, Contreras-Martel C, Pelicic V, Dessen A. 2008. Structure of a widely conserved type IV pilus biogenesis factor that affects the stability of secretin multimers. *J Mol Biol* 378:1031–1039. <http://dx.doi.org/10.1016/j.jmb.2008.03.028>.
127. Kelley LA, Mezulis S, Yates CM, Wass MN, Sternberg MJ. 2015. The Phyre2 web portal for protein modeling, prediction and analysis. *Nat Protoc* 10:845–858. <http://dx.doi.org/10.1038/nprot.2015.053>.
128. Yang J, Yan R, Roy A, Xu D, Poisson J, Zhang Y. 2015. The I-TASSER Suite: protein structure and function prediction. *Nat Methods* 12:7–8. <http://dx.doi.org/10.1038/nmeth.3213>.
129. Kim DE, Chivian D, Baker D. 2004. Protein structure prediction and analysis using the Robetta server. *Nucleic Acids Res* 32:W526–W531. <http://dx.doi.org/10.1093/nar/gkh468>.
130. Collins RF, Hassan D, Karupiah V, Thistlethwaite A, Derrick JP. 2013. Structure and mechanism of the PilF DNA transformation ATPase from *Thermus thermophilus*. *Biochem J* 450:417–425. <http://dx.doi.org/10.1042/BJ20121599>.
131. Koo J, Burrows LL, Howell PL. 2012. Decoding the roles of pilotins and accessory proteins in secretin escort services. *FEMS Microbiol Lett* 328:1–12. <http://dx.doi.org/10.1111/j.1574-6968.2011.02464.x>.
132. Nudleman E, Wall D, Kaiser D. 2006. Polar assembly of the type IV pilus secretin in *Myxococcus xanthus*. *Mol Microbiol* 60:16–29. <http://dx.doi.org/10.1111/j.1365-2958.2006.05095.x>.
133. Rumszauer J, Schwarzenlander C, Averhoff B. 2006. Identification, subcellular localization and functional interactions of PilMNOWQ and PilA4 involved in transformation competency and pilus biogenesis in the thermophilic bacterium *Thermus thermophilus* HB27. *FEBS J* 273:3261–3272. <http://dx.doi.org/10.1111/j.1742-4658.2006.05335.x>.
134. Koo J, Tammam S, Ku SY, Sampaleanu LM, Burrows LL, Howell PL. 2008. PilF is an outer membrane lipoprotein required for multimerization and localization of the *Pseudomonas aeruginosa* type IV pilus secretin. *J Bacteriol* 190:6961–6969. <http://dx.doi.org/10.1128/JB.00996-08>.
135. Robert-Paganin J, Nonin-Lecomte S, Réty S. 2012. Crystal structure of an EAL domain in complex with reaction product 5'-pGpG. *PLoS One* 7:e52424. <http://dx.doi.org/10.1371/journal.pone.0052424>.
136. Navarro MV, De N, Bae N, Wang Q, Sondermann H. 2009. Structural analysis of the GGDEF-EAL domain-containing c-di-GMP receptor FimX. *Structure* 17:1104–1116. <http://dx.doi.org/10.1016/j.str.2009.06.010>.
137. Guzzo CR, Dunger G, Salinas RK, Farah CS. 2013. Structure of the PilZ-FimXEAL-c-di-GMP complex responsible for the regulation of bacterial type IV pilus biogenesis. *J Mol Biol* 425:2174–2197. <http://dx.doi.org/10.1016/j.jmb.2013.03.021>.
138. Li TN, Chin KH, Liu JH, Wang AH, Chou SH. 2009. XC1028 from *Xanthomonas campestris* adopts a PilZ domain-like structure without a c-di-GMP switch. *Proteins* 75:282–288. <http://dx.doi.org/10.1002/prot.22330>.
139. Kim K, Oh J, Han D, Kim EE, Lee B, Kim Y. 2006. Crystal structure of PilF: functional implication in the type 4 pilus biogenesis in *Pseudomonas aeruginosa*. *Biochem Biophys Res Commun* 340:1028–1038. <http://dx.doi.org/10.1016/j.bbrc.2005.12.108>.
140. Buensuceso RN, Nguyen Y, Zhang K, Daniel-Ivad M, Sugiman-Marangos SN, Fleetwood AD, Zhulin IB, Junop MS, Howell PL, Burrows LL. 2016. The conserved tetratricopeptide repeat-containing C-terminal domain of *Pseudomonas aeruginosa* FimV is required for its cyclic AMP-dependent and -independent functions. *J Bacteriol* 198:2263–2274. <http://dx.doi.org/10.1128/JB.00322-16>.